

Energy Efficiency Performance Evaluation of Back-Pressure Driven Cooperative Relay Selection for WiMAX Systems

Mahmoud Hadeif
Samsung Electronics
Research Institute, SEUK
United Kingdom

Apostolos Apostolaras
Centre for Research and
Technology Hellas, CERTH
University of Thessaly
Greece

Alain Mourad
Samsung Electronics
Research Institute, SEUK
United Kingdom

Jim Oreilly
Samsung Electronics
Research Institute, SEUK
United Kingdom

Iordanis Koutsopoulos
Centre for Research and
Technology Hellas, CERTH
University of Thessaly
Greece

Thanasis Korakis
Centre for Research and
Technology Hellas, CERTH
University of Thessaly
Greece

Leandros Tassiulas
Centre for Research and
Technology Hellas, CERTH
University of Thessaly
Greece

ABSTRACT

This paper proposes an energy efficient buffer-level aided relay selection mechanism for mobile communication networks that is based on the back-pressure algorithm. The mechanism exploits channel state information and the availability of buffers at the relays to perform dynamic relay selection based on an analytical framework derived from a Lyapunov optimization. The latter ensures a maximization of the cell throughput while preserving the stability of backlog queues. Performance evaluation is conducted using a WiMAX System Level Simulator compliant with IEEE 802.16m standard and supports various relaying scenarios. In order to represent the system energy efficiency of the whole WiMAX system, a sophisticated and holistic energy consumption model that maps the RF output power radiated at the antenna elements of each node on the network to the total supply power of the node equipment is implemented. Two derivatives of the proposed mechanism for half duplex and full duplex systems are proposed and evaluated. Preliminary results on the Above Roof Top relaying scenario reveal a noticeable increase on both cell throughput and system energy efficiency, in terms of joules per bit, compared to conventional relaying protocols.

Keywords

Wireless relay network, energy efficiency, relay selection, buffer-aided, throughput, diamond topology, WiMAX.

Permission to make digital or hard copies of all or part of this work for personal or classroom use is granted without fee provided that copies are not made or distributed for profit or commercial advantage and that copies bear this notice and the full citation on the first page. To copy otherwise, to republish, to post on servers or to redistribute to lists, requires prior specific permission and/or a fee.

EMUTools 2013 March 5th, Cannes, France.

Copyright 2013 ACM X-XXXXX-XX-X/XX/XX ...\$15.00.

1. INTRODUCTION

Energy consumption in mobile communication networks has swiftly shifted from the state of low priority to a centre of attention within the telecommunication community. The increased network running costs from an operator's perspective, government legislation and energy targets, added to an unprecedented awareness in society on the dramatic impact of excessive energy consumption on global warming, are key drivers for improving energy efficiency in mobile network operations [1]. As a technology enabler, relaying has re-emerged over the past half-decade not only to provide coverage extension but also for its ability to alleviate fading in wireless channels by introducing spatial diversity and for its capability to improve overall system energy efficiency for mobile networks. Energy efficiency is a critical line item in infrastructure wireless networks since it affects wireless operator's budget and functional costs. Large energy costs for operating an infrastructure network need sophisticated methods for reducing the energy consumption while also meeting the increasing consumer demands. Focusing on relaying techniques, where relays are part of the infrastructure, can aid jointly in improving network's universal coverage and energy efficiency. In this work, we primarily study relaying techniques for infrastructure wireless networks, and we elaborate them for evaluation in a system-level simulator in the emerging WiMAX field.

1.1 Related Work

The conventional three node relay model was initially proposed by Van Der Meulen in [2], and Cover and El Gamal in [3] investigated the capacity of a memory-less full-duplex relay channel. Multi-relay-assisted communication has gained significant momentum during the last decade and has been actively studied and considered in the standardization process of state of the art mobile broadband communication systems such as 4G LTE-Advanced and WiMAX IEEE 802.16m [4].

The seminal work of Tassiulas [5] established a framework for indicating throughput optimal scheduling in radio

networks by introducing the well known back-pressure algorithm that exploits queueing backlogs as system state information to derive an optimal scheduling policy. As an enhancement of the previous works Neely in [6] developed a dynamic control strategy for minimizing energy expenditure in a time varying wireless network with adaptive transmission rates. The algorithm operates without knowledge of traffic rates or channel statistics, and yields average power that is arbitrarily close to the minimum possible value achieved by an algorithm optimized with complete knowledge of future events. The aforementioned works set up the foundation for creating a concrete framework [7, 8] for resource allocation in several wireless network types. This framework uses the well known Lyapunov-drift technique relying on concrete mathematical optimization analysis to describe networking actions and performance efficiency towards a certain optimization objective.

Berry et al. in [9, 10] study cooperative communication models that incorporate stochastic traffic arrivals for multiple sessions as well as the related queuing dynamics in all network nodes. These works employ the *Decode-and-Forward* (DF) relaying technique, in which all cooperating nodes must decode a packet before forwarding it. A two-hop diamond network topology is considered for evaluation purposes, where N relays act as intermediary nodes for forwarding the traffic for a particular source-destination pair, and a half-duplex communication constraint is also imposed. The goal is to propose a throughput optimal policy that stabilizes the network for any arrival rate in its stability region. An important assumption is that for a packet to be transmitted over a cooperative link, it must have been previously received through one of the corresponding broadcast links. This assumption implies that each packet is present at each cooperative set of nodes. The works of Berry does not consider a generic optimization framework as in [5, 6, 7, 8] rather than focusing solely on maximizing the throughput of a wireless cooperative network. In our work, we inspired by the Lyapunov optimization in order to extend Berry's work and to establish a framework that will be used for improving of a cooperative network's performance for a certain power-objective while also attaining a performance-delay tradeoff.

In multi-relay networks, relay selection techniques are simple to implement and can attain the same diversity order as more complex schemes employing space time block coding [11] or requiring orthogonal channels [12]. The majority of these selection mechanisms such as [13, 14] do not take advantage of buffers at relays and commonly behave with the selected relay receiving data from the source in one time slot and forwarding it in the subsequent slot. The most common scheme on this direction is a relay selection algorithm based on a max – min fairness criterion [13]. In this paper, we adopt a similar technique to the latter for the sake of performance benchmarking.

On the other hand, several state-of-the-art selection techniques such as max – max [15] and adaptive link selection algorithm [16] give relays the freedom to decide on which time slot to receive and on which time slot to transmit packets. This capability requires the relays to have embedded buffers which enable them not to transmit data if the channel condition is poor and hold until better access channel conditions occur. However, these buffer aided techniques may suffer from either severe data delivery delays and/or backlog queue stability issues such as overflow and underflow incidents [16].

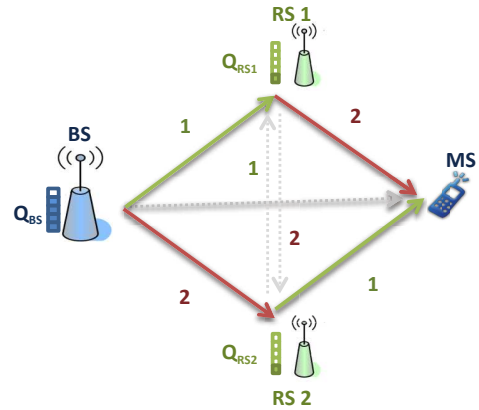


Figure 1: System model of cellular diamond topology comprising one source, two relays, and one destination.

1.2 Our Contribution

In this study we propose a relay selection mechanism which exploits transmission queue lengths and channel quality using Lyapunov optimization in order to maximize throughput and ensure data queue stability at relays. This mechanism initially developed and implemented for WiFi systems in the NITOS wireless testbed [17] showed promising performance gain. The contributions of this paper are as follows:

- In [17], we explored driver implementation issues for a back-pressure driven relay selection policy in a Wi-Fi network that chooses from a set of non-interfering links. However, in this paper, we customized the latter mechanism to leverage the fairness of a centralized scheduler through a system level simulator of a WiMAX network on which both interfering and non-interfering scenarios are considered.
- We explore its potential enhancement not only in terms of throughput and stability but from an energy efficiency perspective as well.
- We implement two derivations of the relay selection algorithm into a WiMAX System Level Simulator developed by Samsung Electronics UK (SEUK) [18].
- We implement the Above Rooftop (ART) relaying scenario which is a diamond topology with 2 relays assigned for each base station.

The first developed derivation obeys a WiMAX half-duplex relay/access links restriction and on the second derivative we introduce some changes to the system in which relays are allowed to transmit data to the destination even though other relays from the same sector are receiving data at the same time slot (The restriction that the same relay is not allowed to transmit and receive at the same time is still maintained). In order to quantify the energy efficiency of the wireless network, the power consumption of the entire system needs to be captured in a well defined framework. For this purpose the holistic framework developed in the EU FP7 EARTH project is adopted and modified accordingly to support the WiMAX system [19]. The latter framework has a flexible and sophisticated model of energy consumption within which all components and sub-components of the whole network system are considered.

In the remainder of this paper we first give a system model description of the diamond topology adopted in this study. Then we analyze network performance by specifying the Lyapunov optimization framework and deriving the optimal scheduling policies. Next we present the energy consumption framework used including base station and relay models and explain how Power consumption is estimated at variable loads. Then we describe the WIMAX IEEE 802.16m system level simulator utilized to carry out the performance evaluation. The results of the two relay selection mechanisms developed within the context of this work in terms of capacity, power consumption and energy efficiency are discussed. Finally, we draw our conclusions and present some prospects for future work.

2. SYSTEM MODEL

We consider the two-hop diamond cellular network depicted in Figure 1 consisting of a source node (base station BS), two relay stations RS_1 and RS_2 , and a destination node (mobile station MS). We assume BS , RS_1 , and RS_2 are equipped with buffers with unlimited storage capacity. We denote $Q_{BS}(t)$, $Q_{RS_1}(t)$, and $Q_{RS_2}(t)$ as the corresponding data queue lengths to be transmitted at each node for a given time slot t . We assume that the transmission is organized in packets and the channels are constant for the duration of one time slot and vary independently from one time slot to the next. We also make the following assumption

- Packet injection in the network takes place only on the source node BS with some rate R .
- All other nodes receive intra-network traffic.

Data is delivered to queueing buffers located in each node i that belongs in the set of cooperative network nodes $\mathcal{N} = \{BS, RS_1, RS_2, MS\}$, for transmission over the wireless links. Let us also define by \mathcal{N}_{in} the set of nodes from which node i receives internal traffic, and \mathcal{N}_{out} the set of nodes that node i transmits. The queue backlog evolves according to the following equation:

$$Q_i(t+1) = [Q_i(t) - \sum_{b \in \mathcal{N}_{out}} R_{ib}(t)]^+ + A_i(t) + \sum_{a \in \mathcal{N}_{in}} R_{ai}(t), \quad (1)$$

where $[\cdot]^+$ denotes the $\max(\cdot, 0)$ and $A_i(t)$ are the exogenous arrivals on node i at time slot t (as previously mentioned, only the source node (base station BS) receives exogenous arrivals in the network). The transmission rate $R_{ab}(t) = R_{ab}(\mathcal{S}_{ab}(t))$ in the link (ab) on slot t depends on the link channel state condition $\mathcal{S}_{ab}(t)$ and it is determined by the transmission power and the channel condition. We assume that the channel state $\mathcal{S}(t)$ is known at the beginning of each time slot t and remains constant over its duration, but it can be variable throughout time slots. $\sum_a R_{ai}(t)$ refers to the cumulative internal traffic arriving at node i at time slot t and $\sum_b R_{ib}(t)$ is the traffic served from node i to all other nodes at slot t .

The two relays RS_1 and RS_2 assist the source node BS whenever channel conditions (or other factors such as queue congestion) do not favor direct source-destination transmission by carrying out traffic through alternative links. In fact, on this model we follow a simple rule to associate the serving node to MS . If the Signal to Interference plus Noise Ratio (SINR) of the direct link $BS - MS$ is superior to both $RS_1 - MS$ and $RS_2 - MS$ links no relays are used and only

the direct link is scheduled to carry out data transmission at that time slot, otherwise cooperative relay assisted transmission is considered.

For relay assisted transmission, we consider two transmission protocols, the half duplex and full duplex scheduling. For half duplex the relay links $BS - RS_1$ and $BS - RS_2$ and the access links $RS_1 - MS$ and $RS_2 - MS$ are interference free and impose the constraint that, at any time slot t , either access links or relay links are activated at a time. In full duplex both links $BS - RS_1$ and $RS_2 - MS$ or $BS - RS_2$ and $RS_1 - MS$ can operate simultaneously. Note that in full duplex the same node is still not allowed to transmit and receive at the same time slot. In other words $BS - RS_1$ and $RS_1 - MS$ or $BS - RS_2$ and $RS_2 - MS$ cannot be performed simultaneously. The full duplex scheme will ensure transmission of extra packets compared to half duplex but with the cost of introducing interference at the receiving node (either MS or RS) from simultaneously transmitting nodes which could either BS or RS , as depicted by grey dotted links in Figure 1. In order to activate the feasible schedules each time slot t , we assume the existence of a system controller $\mathbf{a}(t)$ that chooses between pair 1 and pair 2, by setting $\mathbf{a}(t) = 0$ when pair 1 is to be activated and $\mathbf{a}(t) = 1$ for pair 2.

We assume that the source node BS has access to Channel State Information (CSI) of all links and is responsible for selecting the relays for transmission and reception. The BS informs the selected relays via an error-free feedback channel. Next we explore the relay selection rule adopted as a benchmark and the proposed mechanism.

2.1 Diamond Relay Network

The proposed relay selection exploits the availability of buffers and CQI of all links to perform relay selection which maximize the throughput and maintain queue stability at the buffers. The links are activated in pairs to take full advantage of the available data pending for transmission at relays. Therefore, the scheduling is performed by activating either pair 1 (BS, RS_1 and RS_2, MS) or pair 2 (BS, RS_2 and RS_1, MS). The pair transmission can be either performed within one time slot or two slots depending on whether a full duplex or half duplex protocol is adopted.

The rule to be followed to decide whether pair 1 or pair 2 is to be activated is derived from Lyapunov drift [7, 8] and seeks to maximize networks throughput performance by choosing at each time slot t the appropriate schedules. This rule is given by the following metric and its derivation analysis is given in Section 3:

if	$(Q_{RS_1} - Q_{BS}) R_{BS,RS_1} - Q_{RS_2} R_{RS_2,MS} >$
	$(Q_{RS_2} - Q_{BS}) R_{BS,RS_2} - Q_{RS_1} R_{RS_1,MS}$
then	$\mathbf{a}(t) = 0$, Activate Pair 1: $(BS, RS_1), (RS_2, MS)$.
else	$\mathbf{a}(t) = 1$, Activate Pair 2: $(BS, RS_2), (RS_1, MS)$.

3. NETWORK PERFORMANCE ANALYSIS

For the system illustrated in Figure 1, we seek to enable direct transmissions from source node to relays and from

relays to destination in order to aid the networking communication. Given the topology above and considering the channel state and queue size variations, the objective is to designate a joint power control/scheduling policy that determines the operation in the cooperative network with the goal of *maximizing the total throughput* of the network. To this end, we formulate a problem based on Lyapunov drift theory [7, 8] and on the well known back-pressure algorithm [5].

Throughput Maximization: The objective is to select schedules so as to maximize the total traffic rate of the cooperative network. We also impose a per-node power constraint that reflects the maximum transmission power for a single node, however we are interested in selecting schedules each time slot t that will eventually increase the total throughput. An appropriate selection of the tuning parameter V , makes the initial problem of Power Minimization to be reduced to Throughput Maximization. By observing the power minimization formulation, if we set $V = 0$, we get a max-weight scheduling decision algorithm.

The desired tradeoff between the achieved optimization objective and congestion-induced delay can be expressed clearly, by selecting the V parameter value. In the *Power Minimization* case, the objective is to keep the total power consumption low (i.e. to increase the network's lifetime in case of limited power capacity in handheld devices) while also stabilizing the queues. Hence, selection of schedules is done so as to minimize the total power consumption in the cooperative network. The control variable V can be used as a tuning parameter to provide a suitable power optimality-delay tradeoff. Specifically, the analysis suggests that the proposed policy can achieve a total power expenditure arbitrarily close to the optimal value (for sufficiently large V), at the cost of increased queue congestion and a corresponding delay. This is an additional operating characteristic that can be adjusted by the network controller. Moreover, an important characteristic of the derived policy that will become apparent later is that, even though we consider a joint optimization problem, the power allocation and scheduling decisions are eventually decoupled (i.e. we first compute the optimal power allocation for a slot, and then determine the schedule for this allocation).

3.1 Lyapunov Optimization Framework

Let the system state be $\Theta(t) = Q(t)$, and a Lyapunov function that describes the aggregate network congestion be the the sum of squares of queue backlogs:

$$L(\Theta(t)) \equiv \frac{1}{2}\Theta(t)^2 \equiv \frac{1}{2}Q(t)^2. \quad (2)$$

Let $\hat{p}(\mathbf{a}(t))$ be a controllable penalty function of power consumption that depends on the system controller $\mathbf{a}(t)$ and it is equal to $\hat{p}(\mathbf{a}(t)) = \mathbf{a}(t)[P_{BS,RS_1}(t) + P_{RS_2,MS}] + (1 - \mathbf{a}(t))[P_{BS,RS_2}(t) + P_{RS_1,MS}]$. The one-step Lyapunov drift plus penalty expression[7, 8] is bounded by the following expression:

$$\begin{aligned} \Delta(t) + V \mathbf{E}\{\mathbf{p}(t)\} &\leq B + Q_{BS}(t)\lambda_{BS} + V \{ \mathbf{a}(t)[P_{BS,RS_1}(t) \\ &+ P_{RS_2,MS}(t)] + (1 - \mathbf{a}(t))[P_{BS,RS_2}(t) + P_{RS_1,MS}(t)] \} \\ &- Q_{BS}(t) [\mathbf{a}(t)R_{BS,RS_1}(t) + (1 - \mathbf{a}(t))R_{BS,RS_2}(t)] \quad (3) \\ &- Q_{RS_1}(t)(1 - \mathbf{a}(t))R_{RS_1,MS}(t) - Q_{RS_2}(t)\mathbf{a}(t)R_{RS_2,MS}(t) \\ &+ Q_{RS_1}(t)\mathbf{a}(t)R_{BS,RS_1}(t) + Q_{RS_2}(t)(1 - \mathbf{a}(t))R_{BS,RS_2}(t), \end{aligned}$$

where B is a constant value. By minimizing the bound on the above Lyapunov drift expression of Eq. (3) with respect to $\mathbf{a}(t)$, we obtain:

$$\begin{aligned} \mathbf{a}(t) &\left[V (P_{BS,RS_1}(t) + P_{RS_2,MS}(t) - P_{BS,RS_2}(t) - P_{RS_1,MS}(t)) \right. \\ &- Q_{BS}(t) (R_{BS,RS_1}(t) - R_{BS,RS_2}(t)) + Q_{RS_1}(t)(R_{RS_1,MS}(t) \\ &\left. + R_{BS,RS_1}(t)) - Q_{RS_2}(t) (R_{RS_2,MS}(t) + R_{BS,RS_2}(t)) \right] \quad (4) \end{aligned}$$

Solution: We seek to minimize the bound in the Lyapunov drift expression, by appropriately enabling the controller $\mathbf{a}(t)$ to be either 0 or 1 at each time slot t . The solution follows simply, and the network controller indicates performance efficient schedules by setting $\mathbf{a}(t) = 1$ and selecting $\{BS - RS_1, RS_2 - MS\}$ for activation, when the expression of derivative in Eq. (4) is negative ($[\cdot] < 0$), otherwise we set $\mathbf{a}(t) = 0$ and we activate $\{BS - RS_2, RS_1 - MS\}$ transmission links.

- a) $\mathbf{V} = \mathbf{0}$, then power consumption expression is disregarded, and the problem reduces to stabilizing queues. It is indeed the **(maximum throughput)** approach [5] with no consideration for power consumption. (*This policy is adopted and it is under examination throughout this paper.*)
- b) $\mathbf{V} \gg \mathbf{0}$, the power consumption expression dominates all other queuing factors in Eq. (4). The problem is reduced to select only power efficient schedules without any consideration of queuing backlogs.
- c) $\mathbf{0} < \mathbf{V} < \infty$, This is the intermediary regime where we seek to attain a desired a *power-throughput* performance tradeoff. For large values of V the policy selects more power conservative schedules causing larger queues and larger networking delay. For small values of V (close to zero) the power consumption is bigger while the queue congestion falls while also the networking delay is reduced.

3.2 Throughput-Optimal and Power Efficient Control Algorithm

As reported previously, the throughput maximization algorithm is a special case of the power-optimal algorithm when variable $V = 0$ is set to zero. The algorithm reels out in a similar manner with the power-optimal algorithm with the only exception that it does not take into account within the metric formula the power consumption occurring at transmission, since tuning parameter $V = 0$ is equal to zero. However, the maximum throughput algorithm reflects its power efficiency in a per throughput basis since it can achieve lower power consumption for larger amounts of throughput traffic sent, compared with conventional relaying strategies. Of course power-optimal algorithms (that are not in this paper) can achieve even more lower power consumption with a significant cost in delay causing a significant *performance-delay* tradeoff.

4. NETWORK POWER MEASUREMENT FRAMEWORK

A holistic power model that maps the RF output power radiated at the antenna elements (P_{out}), to the total supply power of node equipment (P_{in}) as developed within the context of the EARTH project [20], is adopted in this work for the following reasons:

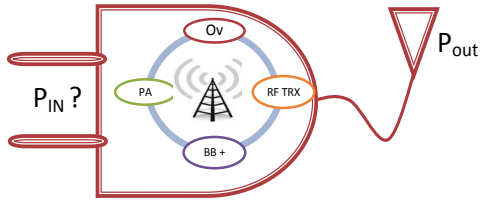


Figure 2: Block diagram of main energy consuming component in *BS* and *RS*.

- Defines a rational interface between the component and system levels.
- Based on a comprehensive modeling of all node components and sub-components (baseband, RF, Power amplifier, Overhead) that contribute into the overall power consumption of the entire radio access network.
- Can be configured to support low load and no load scenarios.
- Takes into account the required energy for the associated baseband signal processing operations.
- Covers different type of nodes from Micro to Femto stations and provides approximate figures of energy consumption for relay nodes.
- Shows good flexibility in terms of how power figure scales with various system parameters such time and frequency cycling, bandwidth, coding rate, number of antennas, and modulation scheme.

Note that the EARTH model is primarily designed based on the 4G LTE system specification [19]. Some changes are required to support the WiMAX system. The changes made are manageable thanks to the two systems similarities and the model flexibility and granularity. The changes are mainly related to relay modeling and will be illustrated in due course.

4.1 Flexible Power Modeling of WiMAX

This section attempts to summarize at high-level the flexible model used in this work. The model considers all nodes which are involved in a transmission (*BS*, *RS* and *MS*). Even though the *MS* power can be modeled using the same framework, to a certain extent, it is omitted on this study for simplicity reasons. The focal point is on *BS* and *RS* nodes consumption. Figure 2 exhibits a simplified block diagram of different components of *BS/RS* node which contribute to the total dissipated energy. Each node is made of multiple transceivers with multiple antennas. Each of these transceivers comprises a Power Amplifier (PA), a Radio Frequency (RF) small-signal transceiver section, a baseband interface (BB) and an overhead power. The overhead is produced from the DC-DC power supply, active cooling system and finally the main AC-DC power supply for connection to the electrical power grid Eq. (5) Note that active cooling is only relevant for the *BS* and it is neglected in the *RS*. Therefore, the total consumed power can be given as:

$$P_{Total} = P_{BB} + P_{RF} + P_{PA} + P_{Overhead} \quad (5)$$

The EARTH approach showed that both baseband as well as RF power consumption are scalable figures and can be modeled under the same form.

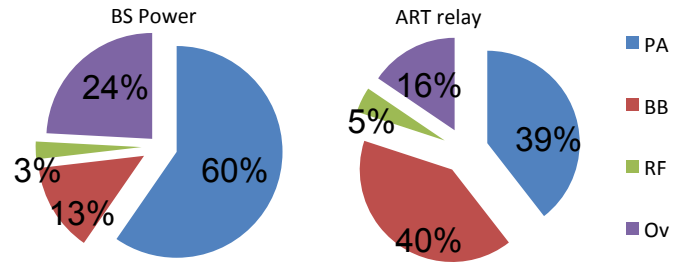


Figure 3: Percentage share node components for *BS* and *ART RS*.

4.2 Power Consumption at Maximum Load

By utilizing the above consumed power of each sub-component we can figure out the total power dissipated by the node for maximum load. For reference values of the system configuration parameters defined in Eq. (5) the breakdown and the total power of both WiMAX *BS* and *ART RS* is obtained and summarized in Table 1.

Table 1: Base and relay station power consumption at maximum load as 65nm CMOS technology for downlink scenario.

	<i>Node Components</i>	<i>Units</i>	<i>Base Station</i>	<i>ART Relay Station</i>
PA	Max Tx Power	[dBm]	46.0	36
	P_{max} (average)	[W]	20.0	4
	Feeder loss	[dB]	-3.0	0
	Back-off	[dB]	8.0	8.0
	Max PA out	[dBm]	54.0	44
	PA efficiency	[%]	31.1	15.5
	Total PPA	[W]	128.6	25.7
Overhead	Total BB	[W]	29.2	26.4
	Total RF TX	[W]	5.8	2.9
	η_{dc}	[%]	7.5	7.5
	η_{cool}	[%]	10	0.0
	η_{ac}	[%]	9	9.0
	Total Overhead	[W]	52.1	10.1
	Total power per TRX	[W]	215.6	65.1

As can be seen from Figure 3, the majority of the power consumption for the base station comes from power amplifiers (PAs) with around 60% of the total *BS* consumed energy. While WiMAX *BS* power consumption is strongly dominated by PA and to a lesser extent by the overhead power with a percentage of 24%, the *ART station* is less PA-dominated and shows significant baseband share of 40%.

4.3 Power Consumption at Varying Load

The node load is defined by P_{out}/P_{max} which is proportional to the amount of utilized resources, comprising both

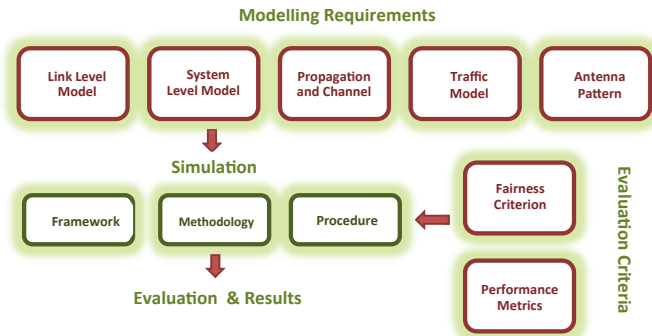


Figure 4: WiMAX system level simulator architecture.

data and control signals. Examination of the node power consumption as a function of its load reveals that mainly the PA scales with the load. However, this scaling over signal load largely depends on the node type. While the power consumption P_{in} is load-dependent for the macro BS the dependency is to lesser extent. The reason is that for the ART relay, the PA accounts for less than 40% of the overall power consumption, whereas for macro BS the PA power consumption amounts to 60 percent of the total, which mandates more sophisticated PA architectures for the latter. Hence, a linear approximation of the node power model appears justified:

$$P_{Total} = N_{TRX}P_0 + \Delta_p P_{out}, \quad P_{out} \leq P_{max} \quad (6)$$

Where P_0 is the power consumption at the minimum non-

Table 2: Power model parameters for different node types at variable load.

Node Type	$P_{max} (W)$	$P_0 (W)$	Δ_p
Base Station	20	130	4.7
Relay Station	4	50.4	3.65

zero output power, and Δ_p is the slope of the load-dependent power consumption. The parameters of the linear power model of Eq. (6) for BS and ART RS are obtained by least squares curve fitting and are listed in Table 2.

4.4 Energy Per Bit Metric

The energy per bit metric is defined as the average network energy consumption (E) during the observation period (T) divided by the average number of bits (B_t) that were correctly delivered in the network during the same time period and is expressed in $[W/bps]$.

$$EPB = \frac{E}{B_t} = \frac{P}{R} \left[\frac{j}{bit} \right]. \quad (7)$$

This energy metric is one of the most commonly used, especially for theoretical studies and single link evaluations. The energy per bit metric looks at the amount of energy spent per delivered bit and is hence an indicator of network bit delivery energy efficiency, which may be important especially in scenarios where the traffic load is high [19]. In this work the energy per bit is the metric we use to evaluate the energy efficiency of the proposed mechanisms.

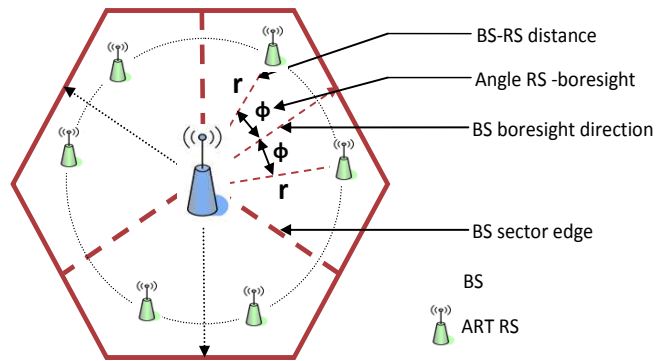


Figure 5: Cell structure for ART scenario.

5. SYSTEM LEVEL SIMULATOR

The platform selected on this work to carry out the energy efficiency evaluation is a system level simulator of the WiMAX standard [21]. On top of energy efficiency the system level evaluation has been extensively used to quantify the benefits of air interface technologies on the global system performance such as the system capacity, throughput, spectral efficiency, and coverage. At the system level, multiple links between multiple transmitters and receivers are considered in a multi-cellular environment, as opposed to the link level, where only the link between a transmitter and a receiver is considered.

On the other hand, the system level integrates upper layer mechanisms for resources allocation and management, whilst accounting for the specificity of the physical layer through the so-called link to system interface. The benefits of physical layer and upper layer mechanisms are quantified on the system performance, primarily in terms throughput, delay, capacity, and coverage. The system level evaluation is essential to promote air interface technologies in standardization, as it quantifies their ultimate benefits on the overall system performance [18]. Like any simulator, the SLS performance is expected to show certain degree of deviation from real system or emulator performance. A combination of accurate calibration and practical transmitter/receiver impairments and implementation losses modelling such as channel estimation errors (caused for example by channel fluctuations during one slot transmission) can close the gap to a tolerable level so that SLS can be considered as an applicable representative of real systems

The system level simulator (SLS) we have built on has been originally developed by SEUK within a previous FP7 project DAVINCI [18] and upgraded to support relays within the context of this project. The developed SLS follows the guidelines provided by the evaluation methodology document [22] and system description document [21] and is compliant with the WiMAX IEEE 802.16m. The SLS is developed for the downlink only and its components are depicted in Figure 4. The core SLS, excluding relaying capabilities, has been embraced by the Samsung Standard Team and has been extensively validated during the DAVINCI project and through cross performance comparison and peer-to-peer validation processes amongst the other standard consortium partners. On the other hand, relaying capabilities have been only validated within the context of this project through

Table 3: Main SLS configuration parameters.

<i>Parameter</i>	<i>Value</i>
Site-to-Site distance	1.5 Km
Number of cells	19
Wrap-around	Yes
Number of sectors per cell	3
Minimum distance to BS	35m
BS maximum transmit power	46dBm
BS antenna maximum gain	17dBi
BS antenna beam width 3dB	70 deg
BS antenna front-to-back ratio	20 dB
MS antenna maximum gain	0dBi
MS receiver noise figure	7dB
MS receiver cable loss	0dB
MS Thermal noise density	-174dBm/Hz
Building Penetration loss	10 dB
Carrier frequency	2.5GHz
Nominal channel bandwidth	10MHz
Number of used subcarriers	721
Cyclic prefix ratio	1/8
Frame duration	5ms
Number of sub-frames	8
DL:UL ratio	5:3
TTG time	102.857 μ s
RTG time	62.857 μ s
Number of sub-carriers/ RU	18
Number of RU	40
PF scheduler latency /time	5ms
PF scheduler latency / RU	10RU
AMC FER threshold	0.01

modular checking processes in an autonomous fashion.

In order for the system level simulator (SLS) to quantify the benefits of the WiMAX system it needs a full set of link performance lookup tables for different codeword sizes, code rates, and modulation schemes. This is in order to properly account for the performance of different resource allocations and physical layer configurations decided by the scheduler, which is the heart of any SLS [18].

5.1 Relaying Support

The WiMAX evaluation document described three-relaying scenarios from which only Above Roof Antenna (ART) is considered in our evaluation at this stage. The ART *RS* scenario as shown in Figure 5 assumes that the *BS* and *RS* are located above rooftop while the *MS*s are located below rooftop (BRT). In ART *RS* scenario a directional narrow-beam donor antenna is used at the *RS*s for the *BS* – *RS*

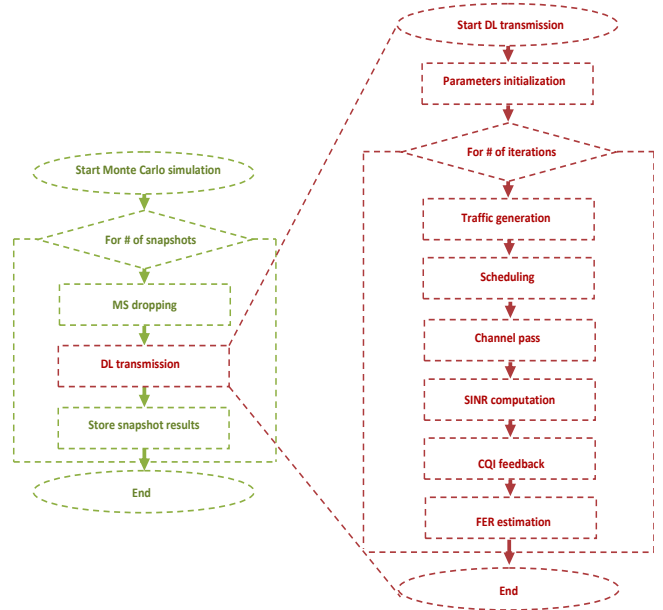


Figure 6: SLS simulation procedure diagram.

link. These antennas are pointed directly to the *BS*. For *RS* – *MS* communication the *RS* uses omni-directional antennas.

In this scenario two *RS*s are deployed in each sector. The positions of the relays are determined by the *BS* – *RS* distance r and the angle ϕ between the boresight direction of the *BS* sector antenna and the LOS to the *RS*. By default the distance r is equal to 3/8 of the site-to-site distance and the angle ϕ is 26 degrees. A directional narrow-beam donor antenna is used at the *RS*s for the *BS* – *RS* link. These antennas are pointed directly to the *BS*. For *RS* – *MS* communication the *RS* uses omni-directional antennas.

The relaying model implemented is defined as a decode, store, encode, forward model. It is assumed that data transmitted on a relay link is decoded and potentially stored until a later frame. It is then encoded and transmitted on the next hop. *MS* associations are static for the duration of one snapshot trial. An *MS* is assigned to associate with one or more of the *BS* and *RS*s in a sector and this association is not changed during a trail. Access link transmissions from/to the *BS* and *RS*s within a sector occur on the same frequency but different times so-called relay and access times. The scheduler adopted is proportional fair centralized scheduling where *BS* takes care of the allocation of resources within its sector.

5.2 SLS Configuration Procedure

The main values of SLS configuration parameters are depicted in Table 3. Figure 6 depicts the functional flowchart of the SLS simulation. This consists of a first loop on the number of snapshots where a given realization of *MS* dropping in the service area is generated, and a second loop where the Down Link (DL) transmission for the different active links is simulated.

The DL transmission first initializes parameters associated with the transmission period (e.g. initial CQI values, initial average throughput, frequency noise generators,

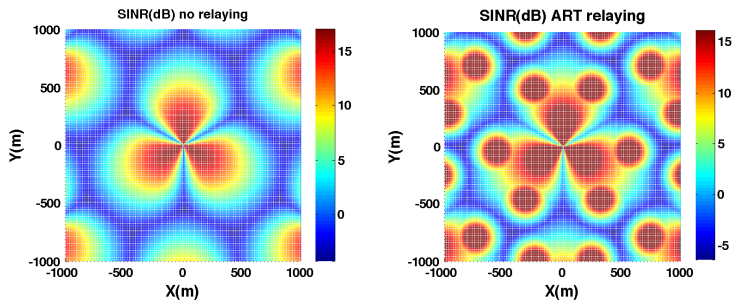


Figure 7: 2D SINR contour map of both non cooperative and cooperative WiMAX.

etc.). It then starts transmission frame per frame following the frame structure defined in the configuration and TDD duplex parameters. The traffic generation is first updated. Then the scheduler of each sector takes the decision regarding which resource units to be assigned to which active *MS* at which modulation and coding schemes. The transmission is then modeled by the channel pass, which first generates the fast fading physical channels for the links between the *MS* and its serving sector and dominant interfering sectors. The physical channels are then transformed into equivalent channels according to the sub-channelization configuration (thus performing the physical to logical sub-channels mapping). The *MS* then computes the per data symbol post-processing SINR for the specified MIMO mode and all resource units over the whole bandwidth. It then determines the CQI per logical resource unit for feedback to the scheduler. The *MS* finally uses the link to system interface tables to estimate the Frame Error rate (FER) associated with the current transmission.

To support ART relays the various system parameters need to be considered for all possible extra links *BS – RS*, *RS – RS* and *RS – MS* configurations and Table 4 highlights the ART relay deployment parameters.

6. SIMULATION RESULTS

In this section we evaluate the performance of the two proposed half and full duplex buffer aided relay selection mechanisms. For this purpose we utilize the above developed WiMAX system level simulator. The utilized network topology is a 19 hexagonal cell layout where each cell is divided into three sectors. Each sector is associated by one macro *BS*. The ART relaying scenario is adopted where two relays are deployed per sector as described in the previous section. We consider the following main simulation parameters: 20 users per sector, 3 snapshots, and transmission of 50 frames per snapshot.

Figure 7 represents the average SINR over 2D area covered by a WiMAX cell in two configurations with and without ART *RS*s. As can be seen *RS*s deployment improved network coverage on cell edges by providing higher average SINRs compared to the non cooperative system on which no relays deployed.

Now we examine four relaying mechanisms using the same simulation configuration and assumptions described above. On the first mechanism no dynamic relay selection is used and *MS*s are associated with the same serving node either *BS* or *RS* for the whole transmission period, basically no

Table 4: ART Relay deployment configuration.

<i>Deployment Parameter</i>		<i>Value</i>	
Number of RS per sector		2	
RS placement distance (r)		3/8 site-to-site distance	
RS placement angle ()		26 degrees	
		Relay L	Access L
RS transmit power	maximum	36dBm	36dBm
Relay station antenna height		32m	32m
Number of tr. antennas		1	2
Number of receive antennas		1	2
Antenna type		Directional	Omni
Antenna gain (boresight)		20 dBi	7dBi
Antenna 3-dB beamwidth		20 degrees	N/A
Antenna front-to-back power ratio		23dB	N/A
Antenna spacing		N/A	4λ
Antenna orientation		Pointed to BS	Pointed to BS
Noise figure		5dB	5dB
Cable loss		2dB	2dB

dynamic relay selection is performed. For the second technique we deploy the conventional relay selection mechanism so-called max – min. In the max – min no Buffer is required and the relay which provides maximum of the minimum channel quality index (CQI) of both *BS – RS* and *RS – MS* is selected [13]. The third approach is the proposed half duplex relay selection (referred in plots by CERTH 1/2 or half duplex) and finally the proposed relaying selection implemented in full duplex mode (referred in plots by CERTH 1/1 or full duplex).

Figure 8 recaps the main results obtained after running the four mechanisms over the three snapshots and demonstrates the coverage, capacity, power consumption and energy efficiency of the four mechanisms. The main observations can be summarized as follows:

- As expected, the new mechanism shows a slight increase of around 5% in the average consumed power per cell since it employs two relays to perform transmission compared to the conventional relaying max – min technique which exploits only one at a time. Both half duplex and full duplex proposed mechanisms show quite similar power consumption.

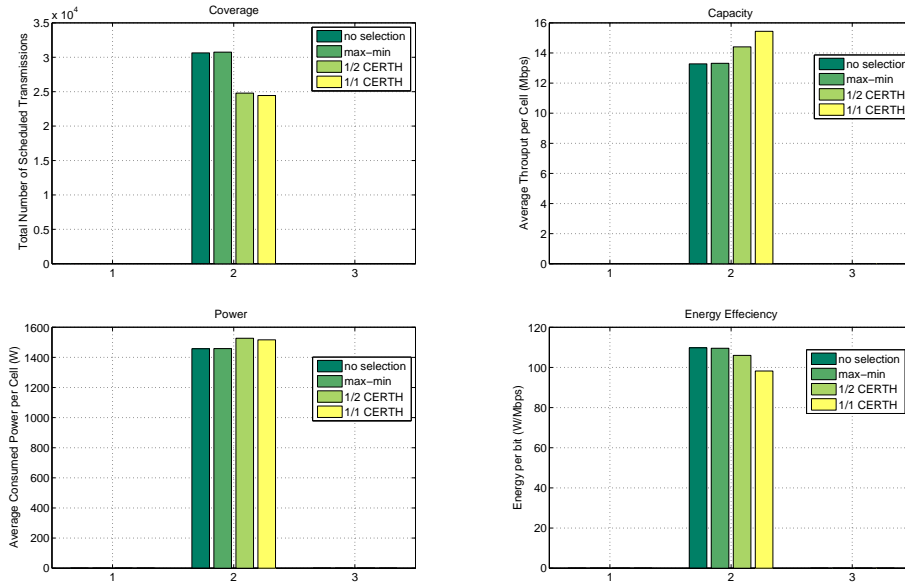


Figure 8: Coverage, capacity, power consumption and energy efficiency evaluation of the proposed relay selection compared to max – min and no dynamic selection protocol.

- From a capacity and throughput perspective a noticeable improvement of around 17% is observed when full duplex relay selection is deployed compared to the conventional max min and to the relaying transmission where no adaptive selection is used. Note that half duplex showed a smaller increase of around 9% compared to the same two techniques.
- Finally from an energy efficiency perspective a gain of 11% in terms of joule per bit is achieved by activating new full duplex relay selection and only around 5% if a half duplex mode is turned on compared to the conventional max – min and no adaptive relay selection protocol.
- The conventional max – min did not show any noticeable enhancement on the ART scenario and this is mainly because both relay links $BS-RS_1$ and $BS-RS_2$ are LOS channels with excellent and identical channel quality.

Finally, Figure 9 and Figure 10 show the above described experiment improvements in terms of cumulative distribution of both capacity and energy efficiency of the new proposed relay selection compared to conventional max – min and with no relay selection protocol.

7. CONCLUSIONS & FUTURE WORK

In this paper, we proposed and evaluated two derivatives of a new relay selection mechanism in a WiMAX system level simulator in terms of energy efficient and throughput. The two mechanisms are half and full duplex buffer aided relay selection techniques derived from Lyapunov drift. A holistic energy consumption model has been implemented to represent the energy efficiency of the cellular network. A gain of around 17% in terms of sector throughput and 11% in terms of energy efficiency have been observed by deploying full duplex mechanism into ART relaying scenario.

Interesting extensions of the presented work include ex-

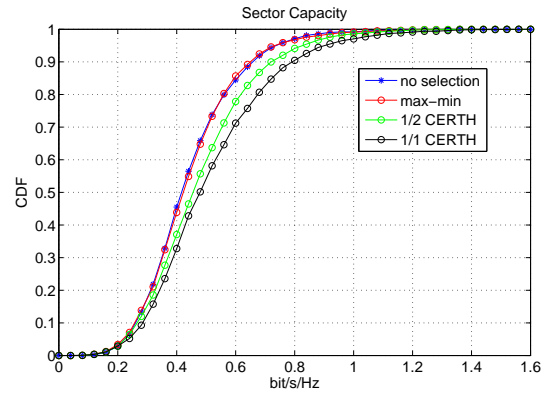


Figure 9: Cumulative distribution of sector capacity of the four relay selection mechanisms.

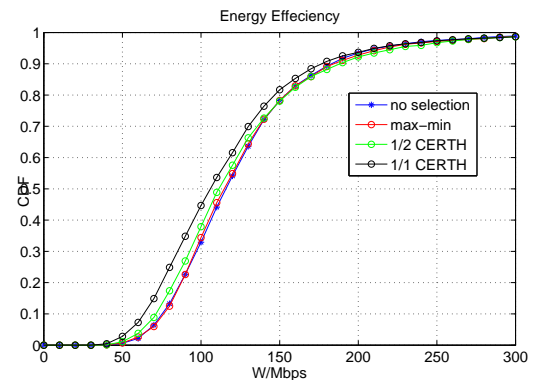


Figure 10: Cumulative distribution of energy per bit of the four relay selection mechanisms.

ploring the performance of the proposed relaying mechanism in more complex diamond topologies on which more than two relays are involved on the cooperative communication between BS and MS in either two-hop or multi-hop fashion. Best WiMAX relaying candidate would be the Below Roof Top (BRT) scenario on which 6 relays are deployed per sector with more dynamic BS-RS channels. The latter renders the system without relay selection mechanism more vulnerable to fading channels whereas the need of robust relaying is more evident. Also possible extension of this work is to incorporate power minimization using the same optimization framework. The objective is to maximize networks lifetime by choosing to minimize total power expenditure while ensuring the system stability with a cost in networking delay. Moreover, an extra benefit of our design approach lies on its generalization potential. The proposed model can be easily implemented into the emerging Long-Term Evolution (LTE) Advanced system since both LTE-A and WiMAX use OFDMA technique for downlink and support reasonably similar relaying capabilities.

8. ACKNOWLEDGMENTS

This work of M. Hedef, A. Apostolaras, T. Korakis and L. Tassiulas was supported and received funding from the European Community's Seventh Framework Programme, CONNECT (FP7/2007-2013) under grant agreement n^o257616. I. Koutsopoulos acknowledges the support of ERC08-RECITAL project, co-financed by Greece and the European Union (European Social Fund) through the Operational Program "Education and Lifelong Learning"-NCRF 2007-2013.

9. REFERENCES

- [1] G. Auer, V. Giannini, C. Desset, I. Godor, P. Skillermark, M. Olsson, M.A. Imran, D. Sabella, M.J. Gonzalez, O. Blume, and A. Fehske. How much energy is needed to run a wireless network? *Wireless Communications, IEEE*, 18(5):40–49, october 2011.
- [2] E. C. van der Meulen. Three-terminal communication channels. *Adv. Appl. Probab.*, 3:120–154, 1971.
- [3] T. Cover and A.E. Gamal. Capacity theorems for the relay channel. *Information Theory, IEEE Transactions on*, 25(5):572–584, sep 1979.
- [4] K. Loa, Chih-Chiang Wu, Shiann-Tsong Sheu, Yifei Yuan, M. Chion, D. Huo, and Ling Xu. Imt-advanced relay standards [wimax/lte update]. *Communications Magazine, IEEE*, 48(8):40–48, august 2010.
- [5] L. Tassiulas and A. Ephremides. Stability properties of constrained queueing systems and scheduling policies for maximum throughput in multihop radio networks. In *Decision and Control, 1990., Proceedings of the 29th IEEE Conference on*, pages 2130–2132 vol.4, dec 1990.
- [6] M.J. Neely. Energy optimal control for time varying wireless networks. In *INFOCOM 2005. 24th Annual Joint Conference of the IEEE Computer and Communications Societies. Proceedings IEEE*, volume 1, pages 572–583 vol. 1, march 2005.
- [7] M. J. Neely. *Stochastic Network Optimization with Application to Communication and Queueing Systems*. Morgan & Claypool Publishers, 2010.
- [8] L. Georgiadis, M. J. Neely, and L. Tassiulas. *Resource allocation and cross-layer control in wireless networks*, volume 1. Foundations and Trends in Networking, 2006.
- [9] E.M. Yeh and R.A. Berry. Throughput optimal control of cooperative relay networks. *Information Theory, IEEE Transactions*, 53(10):3827–3833, oct. 2007.
- [10] Edmund Yeh and Randall Berry. Throughput optimal control of wireless networks with two-hop cooperative relaying. In *Information Theory, 2007. ISIT 2007. IEEE International Symposium on*, pages 351–355, june 2007.
- [11] J. N. Laneman and G. W. Wornell. Distributed space-time-coded protocols for exploiting cooperative diversity in wireless networks. *IEEE Trans. Inf. Theor.*, 49(10):2415–2425, October 2003.
- [12] J.N. Laneman, D.N.C. Tse, and G.W. Wornell. Cooperative diversity in wireless networks: Efficient protocols and outage behavior. *Information Theory, IEEE Transactions on*, 50(12):3062–3080, dec. 2004.
- [13] A. Bletsas, A. Khisti, D.P. Reed, and A. Lippman. A simple cooperative diversity method based on network path selection. *Selected Areas in Communications, IEEE Journal on*, 24(3):659–672, march 2006.
- [14] E. Beres and R. Adve. Selection cooperation in multi-source cooperative networks. *Wireless Communications, IEEE Transactions on*, jan. 2008.
- [15] A. Ikhlef, D.S. Michalopoulos, and R. Schober. Max-max relay selection for relays with buffers. *Wireless Communications, IEEE Transactions on*, 11(3):1124–1135, march 2012.
- [16] N. Zlatanov, R. Schober, and P. Popovski. Buffer-aided relaying with adaptive link selection. *Selected Areas in Communications, IEEE Journal on*, PP(99):1–13, 2012.
- [17] A. Apostolaras, K. Choumas, I. Syrigos, G. Kazdaridis, T. Korakis, I. Koutsopoulos, A. Argyriou, and L. Tassiulas. A demonstration of a relaying selection scheme for maximizing a diamond network's throughput. *Tridentcom 2012*, 2012.
- [18] A. Mourad and Gutierrez I. System level evaluation. *DAVINCI D2.3.1*, INFISO-ICT-216203, 2012.
- [19] A. Auer and Gunther et al. Energy efficiency analysis of the reference systems, areas of improvements and target breakdown. *EARTH D2.3*, INFISO-ICT-247733, 2012.
- [20] C. Desset, B. Debaillie, V. Giannini, A. Fehske, G. Auer, H. Holtkamp, W. Wajda, D. Sabella, F. Richter, M.J. Gonzalez, H. Klessig, I. Godor, M. Olsson, M.A. Imran, A. Ambrosy, and O. Blume. Flexible power modeling of lte base stations. In *Wireless Communications and Networking Conference (WCNC), 2012 IEEE*, pages 2858–2862, april 2012.
- [21] Srinivasan and et al Roshni. Ieee 802.16m system description document (sdd), 2010. IEEE802.16 Broadband Wireless Access Working Group.
- [22] Srinivasan and et al Roshni. Ieee 802.16m evaluation methodology document (emd), 2009. IEEE802.16 Broadband Wireless Access Working Group.